Cheng *et al.*
Protection and Control of Modern Power Systems (2022) 7:46
https://doi.org/10.1186/s41601-022-00265-8

Protection and Control of Modern Power Systems

ORIGINAL RESEARCH Open Access

A novel fault location method for distribution networks with distributed generations based on the time matrix of traveling-waves

Liang Cheng[1], Tao Wang[1,2*] and Yi Wang[1]

Abstract

To improve location speed, accuracy and reliability, this paper proposes a fault location method for distribution networks based on the time matrix of fault traveling waves. First, an inherent time matrix is established according to the normalized topology of the target distribution network, and a post-fault time matrix is obtained by extracting the head data of initial waves from traveling wave detection devices. A time determination matrix is then obtained using the difference operation between the two matrices. The features of the time determination matrix are used for fault section identification and fault distance calculation, to accurately locate faults. The method is modified by considering economic benefits, through the optimal configuration of detection devices of traveling waves when calculating fault distances. Simulation results show that the proposed method has good adaptation with higher fault location accuracy than two other typical ones. It can deal with faults on invalid branches, and the error rate is under 0.5% even with connected DGs.

Keywords: Distribution network, Fault traveling wave, Fault location, Distributed generation

1 Introduction

Electrical power distribution systems are the key connection between power transmission systems and users. A fast and effective fault diagnosis method plays an important role in improving system reliability and ensuring the power quality of users [1]. It is also one of the important foundations for fault isolation and power supply recovery [2].

Therefore when a fault occurs in a distribution network, to restore the power supply in the shortest time a diagnosis method is required to quickly and accurately locate fault points. This can effectively reduce the scope of power line inspection and improve the efficiency of emergency repair [3]. However, since the distribution network usually has a complex topology with numerous branches and large quantities of equipment over an extensive area, it is difficult to accurately identify fault branches and locate fault points [4, 5].

Consequently, much work has been done on the fault location of distribution networks. Many methods have been proposed, such as methods based on impedances [6, 7], fault indicators [8], signal injection [9, 10], traveling waves [11, 12], matrix algorithms [13, 14] and artificial intelligence algorithms [15, 16]. Among them, the traveling wave-based methods are widely used to diagnose faults because of their advantages of high accuracy and fast diagnosis speed. The integration of numerous distributed generators (DGs) leads to variable power flow directions. As a result, it is difficult to effectively identify wave heads at nodes under refraction and reflection of traveling waves by traditional traveling wave-based

*Correspondence: wangatao2005@163.com

[1] School of Electrical Engineering and Electronic Information, Xihua University, Chengdu 610039, China
Full list of author information is available at the end of the article

methods [17, 18]. Consequently, much attention has been paid to improving the existing traveling wave-based methods to increase their handling ability with DGs.

For example, to effectively identify the wave heads of traveling waves, references [19–21] propose identification methods based on the discrete wavelet, continuous wavelet and Hilbert-Huang transforms, respectively, where the high frequency component of single-terminal traveling wave signals is used to locate faults. In [22], a fault location algorithm based on multi-terminal time information is proposed, one which combines single- and double-terminal traveling wave methods. However, it does not consider the fault location of distribution systems with large numbers of branches. In [23], fault branches are located by the differences between the elements of the searching matrix while accurate fault points are determined via a double-terminal traveling wave method. A fault location method for distribution networks is proposed in [24] based on distance matrix and branch coefficient. In this work, the determination matrix for fault branches is established based on the difference between the inherent distance matrix (IDM) before faults and the distance matrix after faults, hence realizing the fault location of branches.

Although above methods effectively promote the development of fault location technology for distribution networks, they require almost all nodes to be installed with traveling wave detection devices. This reduces the economic benefits and is also too idealistic for current engineering practice. Consequently, reference [25] proposes a distributed fault section location method based on the time characteristics of fault transient signals. It considers the optimal configuration of detection devices for travelling waves. The method can accurately locate faulty feeder branches in distribution networks with a limited number of detection devices. Considering the economic efficiency, reference [12] locates faults by the topological information of distribution networks and the traveling wave information generated by returning currents of circuit breakers. The fault distance of distributed feeders is calculated based on the time difference between the coincidence and arrival moment of reflected traveling waves. In [26], wavelet energy entropy is used for fault detection and classification while the wavelet modulus maxima of the line mode component is employed for the accurate location of faults. This work also improves the configuration method of detection devices of traveling waves, so as to effectively and accurately locate faults in networks with multi-branches.

The background of the above methods is quite close closer to real, although they do not fully consider the different wave velocities in overhead lines and cables. Since many distribution networks have overhead line-cable hybrid structures, it is necessary to carefully distinguish the wave velocities in different kinds of lines to further improve the accuracy of fault location. This paper proposes a fault location method based on the time matrix of fault traveling waves for distribution networks. The method has the following features:

- The proposed novel traveling wave-based fault location method of distribution network via the time determination matrix (TDM) has the advantages of simplified computational steps and improved computational efficiency based on the characteristics of matrix elements for different fault types. Both fault locations under the ideal installation and optimal configuration of the detection devices of traveling waves are considered, and therefore the method has good economy and engineering practicability.
- To solve the calculation errors caused by the inconsistent transmission speed of traveling waves in cable and overhead lines, the proposed time determination matrix is calculated and constructed using the normalized traveling wave velocity of overhead lines according to their inherent line parameters. Consequently, the proposed method is well adapted to distribution networks with overhead lines and cables, reducing the online computational complexity while improving computational efficiency and accuracy.
- To improve the accuracy in the identification of faulty invalid branches, an important parameter called the error correction coefficient is introduced. It makes the determination characteristics of the time determination matrix even more obvious. This is critical in determining the valid faulty sections and invalid branches. The elements in the time determination matrix can be used not only for the fault location of sections, but also for the calculation of fault distance. Accordingly, the method is simple and reliable with high robustness.

The remainder of this paper is organized as follows: Sect. 2 proposes an ideal fault location method based on the time matrix of travelling waves. Considering the economic efficiency, a fault location method considering the optimal configuration of detection devices of traveling waves is proposed in Sect. 3. Simulation studies are carried out and the results are provided in Sect. 4. Conclusions are drawn in Sect. 5.

2 Fault location method based on time matrix of fault traveling waves

This section proposes a fault location method based on the time matrix of fault traveling waves in the ideal configuration of detection devices, i.e., all nodes are

equipped with detection devices for traveling waves. Its flowchart is shown in Fig. 1, and the detailed steps are:

Step 1: Normalize the distribution network topology and establish an inherent distance matrix (IDM) before the fault.
Step 2: Establish a pre-fault inherent time matrix (ITM) from the relationship between the IDM and traveling wave velocity.
Step 3: Build a post-fault time matrix by extracting the initial wave head data in the detection devices of traveling waves, hence generating a time determination matrix by the difference operation with the ITM.
Step 4: Use the characteristics of the time determination matrix to identify fault sections, and then the arriving time (i.e., t_f) of wave heads to the ends of fault sections is used to determine whether the fault occurs in the section or at its end.
Step 5: If either t_{f_m} or t_{f_n} equals 0, then the fault occurs at the section end. If and only if t_{f_m} and t_{f_n} are both greater than 0, then the fault occurs in the section.
Step 6: Calculate the fault distance based on the matrix data to obtain the accurate results of fault location.

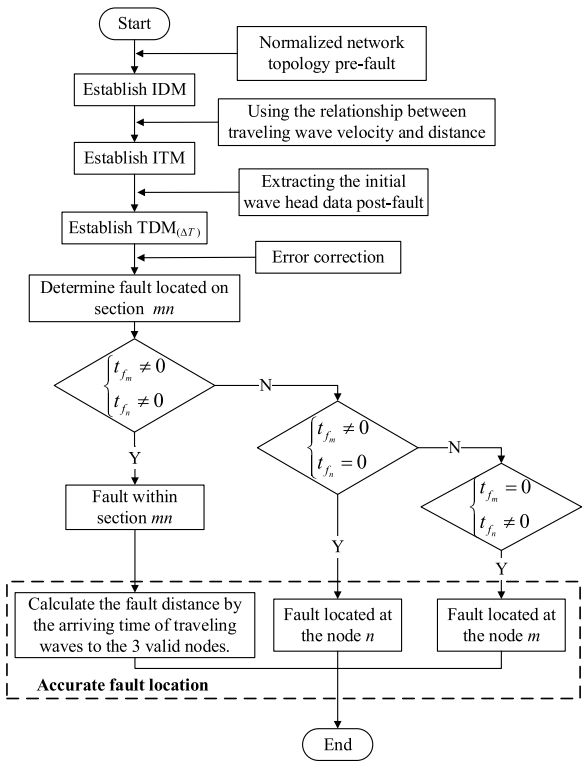

Fig. 1 Flowchart of fault location method under ideal detection device configuration

2.1 Inherent time matrix

In this section, a distribution network with simple topology, shown in Fig. 2, is used to illustrate how to establish an inherent time matrix. In Fig. 2, the nodes marked with symbols $a, b, \ldots, g$ are called valid nodes and are installed with the detection devices of traveling waves. Any two valid nodes make up a valid section, and the distances between them are obtained based on system data, which are represented by $d_{ab}, d_{ac}, \ldots, d_{ag}$, respectively.

If a fault occurs in section m,n $(m,n \in \{a,b,\ldots,g\}$ and $m \neq n)$, the corresponding fault traveling waves will propagate along the line to both valid nodes m and n. Set the arrival times of initial wave heads detected at the valid nodes as $t_{f_a}, t_{f_b}, \ldots, t_{f_n}$, respectively. If the line mode velocity of a traveling wave propagating along the line is v_0, the inherent distance d_{mn} between nodes m and n is:

$$d_{mn} = d_{f_m} + d_{f_n} \tag{1}$$

where d_{f_m} and d_{f_n} satisfy:

$$\begin{cases} d_{f_m} = v_0 * t_{f_m} \\ d_{f_n} = v_0 * t_{f_n} \end{cases} \tag{2}$$

Consequently, d_{mn} can also be calculated by:

$$d_{mn} = v_0 * \left(t_{f_m} + t_{f_n}\right) = v_0 * t_{mn} \tag{3}$$

In general, the distribution networks consist of overhead lines and cables. Because of the different transmission speeds of traveling waves in the two types of lines, large calculation errors can be generated if two different velocities are used in one calculation process. Therefore, to improve computational efficiency and accuracy, we normalize the different speeds to obtain a normalized intrinsic time matrix, which produces a time-determination matrix to locate faults.

The speed parameter expression of a traveling wave is $v=1/\sqrt{LC}$, where L and C represent distributed inductance and capacitance in line mode components, respectively. L and C are largely unaffected by the external environment. Accordingly, the wave velocity v can be regarded as a constant value, and the transmission speeds of traveling waves in overhead lines and cables are expressed as v_1 and v_2 respectively as follows:

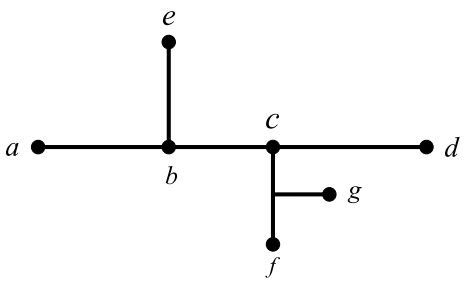

Fig. 2 Simple distribution network topology

$$\begin{cases} v_1 = 1/\sqrt{L_1 C_1} \\ v_2 = 1/\sqrt{L_2 C_2} \end{cases} \tag{4}$$

where L_1 and L_2 represent distributed inductances of overhead lines and cables, respectively, and C_1 and C_2 represent distributed capacitances in the two types of lines, respectively.

Then, the length of a cable in a distribution network can be equivalent to one of an overhead line using their actual physical parameters, as:

$$d^*_{mn} = \frac{d_{mn}}{v_2} * v_1 = \frac{\sqrt{L_2 C_2}}{\sqrt{L_1 C_1}} * d_{mn} \tag{5}$$

where d_{mn} represents the original length of the cable and d^*_{mn} represents the equivalent length.

Based on the equivalent distribution network topology, the inherent distance matrix D^* is given as:

$$D^* = \begin{bmatrix} d^*_{aa} & \cdots & d^*_{ag} \\ \vdots & \ddots & \vdots \\ d^*_{ga} & \cdots & d^*_{gg} \end{bmatrix} \tag{6}$$

Finally, the normalized inherent time matrix T_d can be obtained by D^* and v_0, as:

$$T_d = \frac{D^*}{v_0} = \begin{bmatrix} \frac{d^*_{aa}}{v_0} & \cdots & \frac{d^*_{ag}}{v_0} \\ \vdots & \ddots & \vdots \\ \frac{d^*_{ga}}{v_0} & \cdots & \frac{d^*_{gg}}{v_0} \end{bmatrix} = \begin{bmatrix} t_{aa} & \cdots & t_{ag} \\ \vdots & \ddots & \vdots \\ t_{ga} & \cdots & t_{gg} \end{bmatrix} \tag{7}$$

where $t_{mn} = \frac{d^*_{mn}}{v_0}$, $T^*_d = \frac{D^*}{v_1}$. It is worth noting that T_d is established before the fault and can be modified according to the change of distribution network topology.

2.2 Time determination matrix

Detailed steps for generating a time determination matrix are:

Step 1: Add the time t_{f_m} and t_{f_n} detected at two valid nodes after a fault, hence getting the post-fault time matrix T_f, where $t_{f_m f_n}$ represents the sum of t_{f_m} and t_{f_n}, as:

$$T_f = \begin{bmatrix} t_{f_a f_a} & \cdots & t_{f_a f_g} \\ \vdots & \ddots & \vdots \\ t_{f_g f_a} & \cdots & t_{f_g f_g} \end{bmatrix} \tag{8}$$

Step 2: Take difference calculation between the inherent time matrix and post-failure time matrix, hence getting the time determination matrix ΔT, as:

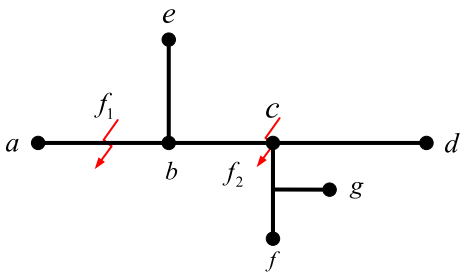

Fig. 3 Failure schematic diagram of simple distribution grid

$$\Delta T = T_f - T_d = \begin{bmatrix} t_{f_a f_a} - t_{aa} & \cdots & t_{f_a f_g} - t_{ag} \\ \vdots & \ddots & \vdots \\ t_{f_g f_a} - t_{ga} & \cdots & t_{f_g f_g} - t_{gg} \end{bmatrix} \tag{9}$$

Step 3: Determine the fault sections based on the relationship between $t_{f_m f_n}$ and t_{mn}. If $t_{f_m f_n} = t_{mn}$, the fault f occurs in the section mn; otherwise, it occurs outside mn. It is worth noting that fault sections are decided by off-diagonal zero elements in the time determination matrix and the diagonal elements will not be used. However, a zero element may become a non-zero element because of external factors in the distribution network, such as line length, electrical parameters and temperatures. In this case, the identification results of fault sections may be wrong. Therefore, Eq. (10) is used to correct the error:

$$\begin{cases} 0, & |x_i| \le \xi \\ x_i, & |x_i| \ge \xi \end{cases} \tag{10}$$

where ξ represents the error correction coefficient, whose value is usually set as 0.005 [27]. x_i is an element in the time determination matrix.

To improve the understandability, two types of faults are employed in the distribution network in Fig. 3, where f_1 occurs in the section ab and f_2 occurs on the valid node c, respectively. Fault sections are identified by the characteristics of elements in the time determination matrix. Based on the detection data of fault traveling waves, the time determination matrix ΔT_1 and ΔT_2 for the fault f_1 and f_2 are obtained respectively, as:

$$\Delta T_1 = \begin{array}{c} \\ a \\ b \\ c \\ d \\ e \\ f \\ g \end{array} \begin{array}{c} \begin{array}{ccccccc} a & b & c & d & e & f & g \end{array} \\ \begin{bmatrix} 0 & 0 & 0 & 0 & 0 & 0 & 0 \\ 0 & 0 & x_1 & x_2 & x_3 & x_4 & x_5 \\ 0 & x_1 & 0 & x_6 & x_7 & x_8 & x_9 \\ 0 & x_2 & x_6 & 0 & x_{10} & x_{11} & x_{12} \\ 0 & x_3 & x_7 & x_{10} & 0 & x_{13} & x_{14} \\ 0 & x_4 & x_8 & x_{11} & x_{13} & 0 & x_{15} \\ 0 & x_5 & x_9 & x_{12} & x_{14} & x_{15} & 0 \end{bmatrix} \end{array} \tag{11}$$

$$\Delta T_2 = \begin{array}{c} \\ a \\ b \\ c \\ d \\ e \\ f \\ g \end{array} \begin{array}{c} \begin{array}{ccccccc} a & b & c & d & e & f & g \end{array} \\ \begin{bmatrix} 0 & x_1 & 0 & 0 & x_2 & 0 & 0 \\ x_1 & 0 & 0 & 0 & x_3 & 0 & 0 \\ 0 & 0 & 0 & x_4 & 0 & x_5 & x_6 \\ 0 & 0 & x_4 & 0 & 0 & x_7 & x_8 \\ x_2 & x_3 & 0 & 0 & 0 & 0 & 0 \\ 0 & 0 & x_5 & x_7 & 0 & 0 & x_9 \\ 0 & 0 & x_6 & x_8 & 0 & x_9 & 0 \end{bmatrix} \end{array} \tag{12}$$

If a fault occurs in section *ab*, according to Eqs. (3) and (9), the values of elements in ΔT_1 referred to section *ab* are equal to 0, and the remaining ones (i.e., $x_1, x_2, \ldots, x_5$) are greater than 0. Here, the related sections include *ab*, *ac*, *ad*, *ae*, *af* and *ag*. From the criterion rule, it is found that the fault section is the common section of related sections. Since $t_{ab}=t_{f_a}+t_{f_b}(t_{f_a} \neq 0, t_{f_b} \neq 0)$, it determines that the fault f_1 occurs in section *ab*.

If the fault occurs at node *c*, according to the same equations and criterion rule, it follows that f_2 occurs in the common sections of *ac*, *ad*, *af*, *ag*, *bc*, *bd*, *bf*, *bg*,*ce*, *de*, *ef* and *eg*, i.e., section *bc*. Since $t_{bc}=t_{f_b}+t_{f_c}$ ($t_{bc}=t_{f_b}, t_{f_c}=0$), the fault f_2 occurs on the node *c* in section *bc*.

2.3 Fault point location

In this section, accurate fault points are located, with the fault f_1 in Fig. 3 taken as an example to illustrate the computational process.

First, the arrival times (i.e., t_{f_a} and t_{f_b}) are obtained when the heads of fault traveling waves reach terminals of the fault section *ab*. The arrival time t_{f_c} is also extracted, where *c* is the valid node of fault traveling waves arriving third. According to t_{f_a}, t_{f_b} and t_{f_c}, it determines that there are two sections (i.e., *ab* and *ac*) containing the fault section *ab*.

Secondly, setting *a* as the reference node, the distance (i.e., the accurate fault location result) from the fault f_1 to node *a* is calculated according to:

$$\begin{cases} d_1 = \frac{t_{f_a}}{t_{f_a}+t_{f_b}} * d_{ab} \\ d_2 = \frac{t_{f_a}}{t_{f_a}+t_{f_c}} * d_{ac} \\ d^* = \frac{d_1+d_2}{2} \end{cases} \tag{13}$$

where d_1 and d_2 represent the distance from the fault point to the reference node *a*, respectively. d^* represents the mean value of d_1 and d_2. Consequently, the accurate fault position is d^* from node *a* in section *ab*. It is worth stating that the average value is taken to improve the accuracy of calculation and reduce error interference.

3 Fault location method under optimal configuration of detection devices

The method proposed in Sect. 2 requires all nodes in a distribution network to be equipped with detection devices, which is neither economical nor realistic in practice. Consequently, a method is required to accurately locate faults while considering the optimal configuration of detection devices. A corresponding method is thus proposed based on the theory in Sect. 2, and its flowchart is shown in Fig. 4. First, the optimal configuration principle of detection devices in distribution networks with an overhead line-cable hybrid structure is presented. The way to locate faults under an optimal device configuration is then introduced.

3.1 Optimal configuration principle of detection devices

Considering economic efficiency, difficulty of line reconstruction and importance of line branches, the

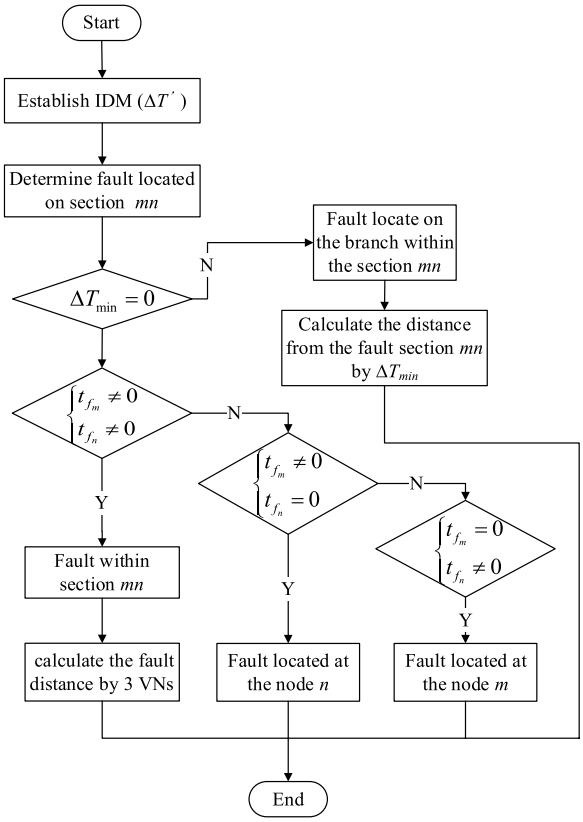

Fig. 4 Flowchart of fault location method considering optimal configuration of detective devices

method in [28] is employed, whose installation principles are:

(a) Terminal nodes of all main feeders should be installed with detection units.
(b) If a node has n adjacent nodes, where more than two are installed with detection units, then the node cannot be configured.
(c) If a node with more than two branches is adjacent to a terminal node, then the node should be configured with detection units.
(d) A connected node of an overhead line and a cable should be installed with detection units.

The above principle is used to optimize the device configuration of the distribution network shown in Fig. 2. The results are shown in Fig. 5, where the dotted and solid lines represent cables and overhead lines respectively. The hollow and solid circles express invalid and valid nodes respectively, and ff_1, gg_1 and hh_1 are sub-branches without detection units. The length of cables is normalized as:

$$d_{be}^{*} = \frac{d_{be}}{v_2} v_1 = \frac{\sqrt{L_2 C_2}}{\sqrt{L_1 C_1}} d_{be} \tag{14}$$

where d_{be} represents the equivalent length of section be to be normalized while d_{be}^{*} indicates the length after normalization.

3.2 Fault location under optimal configuration

In the optimal configuration, it is easy to produce invalid nodes and branches, which are unconfigured detection devices. Therefore, this section makes an adaptive modification of the method proposed in Sect. 2. The basis of the modification is the time determination matrix and the difference lies in the matrix elements. The fault section determination rule under the optimal configuration of devices is:

(a) If $\Delta T'$ obtained in the optimal configuration is still composed of 0 and positive elements, the decision rule for fault sections presented in Sect. 2 can still be adopted. In this case, faults still occur on valid nodes or valid sections.
(b) If all elements in $\Delta T'$ are greater than 0, a fault occurs on an invalid branch. In this case, a fault occurs in a common section of those represented by the same elements with the smallest value in rows and columns of $\Delta T'$.

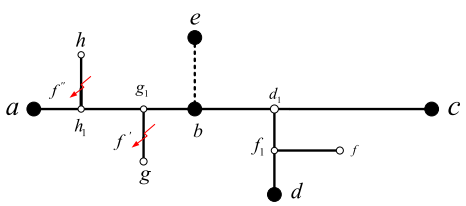

Fig. 5 Schematic diagram of a simple distribution network with overhead line-cable hybrid structure after optimal configuration

In particular, if there is more than one invalid branch in a section, the rule (b) cannot determine the exact invalid branches.

Assuming that faults f' and f'' occur in the distribution network shown in Fig. 5, the corresponding time distance matrices $\Delta T'$ and $\Delta T''$ are:

$$\Delta T' = \begin{array}{c} \\ a \\ b \\ c \\ d \\ e \end{array} \begin{array}{c} \begin{array}{ccccc} a & b & c & d & e \end{array} \\ \begin{bmatrix} 0 & x' & x' & x' & x' \\ x' & 0 & x_1 & x_2 & x_3 \\ x' & x_1 & 0 & x_4 & x_5 \\ x' & x_2 & x_4 & 0 & x_6 \\ x' & x_3 & x_5 & x_6 & 0 \end{bmatrix} \end{array} \tag{15}$$

$$\Delta T' = \begin{array}{c} \\ a \\ b \\ c \\ d \\ e \end{array} \begin{array}{c} \begin{array}{ccccc} a & b & c & d & e \end{array} \\ \begin{bmatrix} 0 & x' & x' & x' & x' \\ x' & 0 & x_1 & x_2 & x_3 \\ x' & x_1 & 0 & x_4 & x_5 \\ x' & x_2 & x_4 & 0 & x_6 \\ x' & x_3 & x_5 & x_6 & 0 \end{bmatrix} \end{array} \tag{16}$$

where x' and x'' represent the smallest positive numbers in $\Delta T'$ and $\Delta T''$, respectively. $x_1, \ldots, x_5$ represent positive numbers greater than x' and x''.From the fault section determination rules in the optimal configuration of devices, it is found that the fault occurs in the common section of sections ab, ac, ad, ae, i.e., section ab. Figure 5 shows that the two faults f' and f'' occur in section ab. However, in this section, there are two invalid branches, i.e., gg_1 and hh_1. Therefore, it is unable to accurately determine that a fault f' or f'' occurs in gg_1 or hh_1.

Consequently, for the above special situation, the determination rule is further presented as follows:

(a) The minimum value $\Delta T_{\min}$ of elements in matrix $\Delta T'$ is obtained by analyzing element characteristics of $\Delta T'$.
(b) It determines the common section where $\Delta T_{\min}$ is located as a fault section. Then, the value of $\Delta T_{\min}$ is used to judge whether the fault occurs in the valid section or on its invalid branch. If $\Delta T_{\min}$ equals 0, the fault occurs in the valid section and the rules described in Sect. 3.1 are also effective; otherwise,

the fault occurs on the invalid branch of the valid section.

(c) Finally, fault positions are located. If the fault occurs in the valid section, the fault point is calculated according to the accurate location method in Sect. 2. If the fault occurs on an invalid branch, the distance from the fault point to the valid section is first calculated according to Eq. (17) shown below. Then, one valid node of the fault section is taken as the reference node, and the distance from the fault point to the reference node is calculated. Consequently, invalid branches are identified by the calculation results compared with the corresponding section length in the inherent distance matrix.

$$d_f = \Delta T_{\min} * v_1 \tag{17}$$

where d_f represents the distance from the fault point to the valid section, i.e., the fault length of the overhead line. If the invalid branch is a cable, the actual electric cable line length is obtained by re-normalizing the length, as:

$$d_f^* = d_f * \frac{v_2}{v_1} \tag{18}$$

where d_f^* is the actual length of the cable.

4 Simulation analysis

In this section, to demonstrate the feasibility and effectiveness of the proposed method, a simulation model is built in the PSCAD environment. A standard IEEE 33 node 10 kV distribution network consisting of overhead line-cable hybrid structures is used for simulation, as shown in Fig. 6a. A simplified diagram is shown in Fig. 6b. Two types of DGs are connected to node b and d, respectively. Section lengths are shown in Table 1, where section *bc* is the equivalent length of a normalized cable. 'Typical' parameters of an overhead line-cable hybrid structure are set by [29]. The velocities of traveling waves in an overhead line and in a cable are calculated as $v_1 = 2.9979 \times 10^5$(km/s) and $v_2 = 1.7209 \times 10^5$(km/s), respectively.

First, a pre-fault inherent distance matrix D is built between any two nodes according to the section length

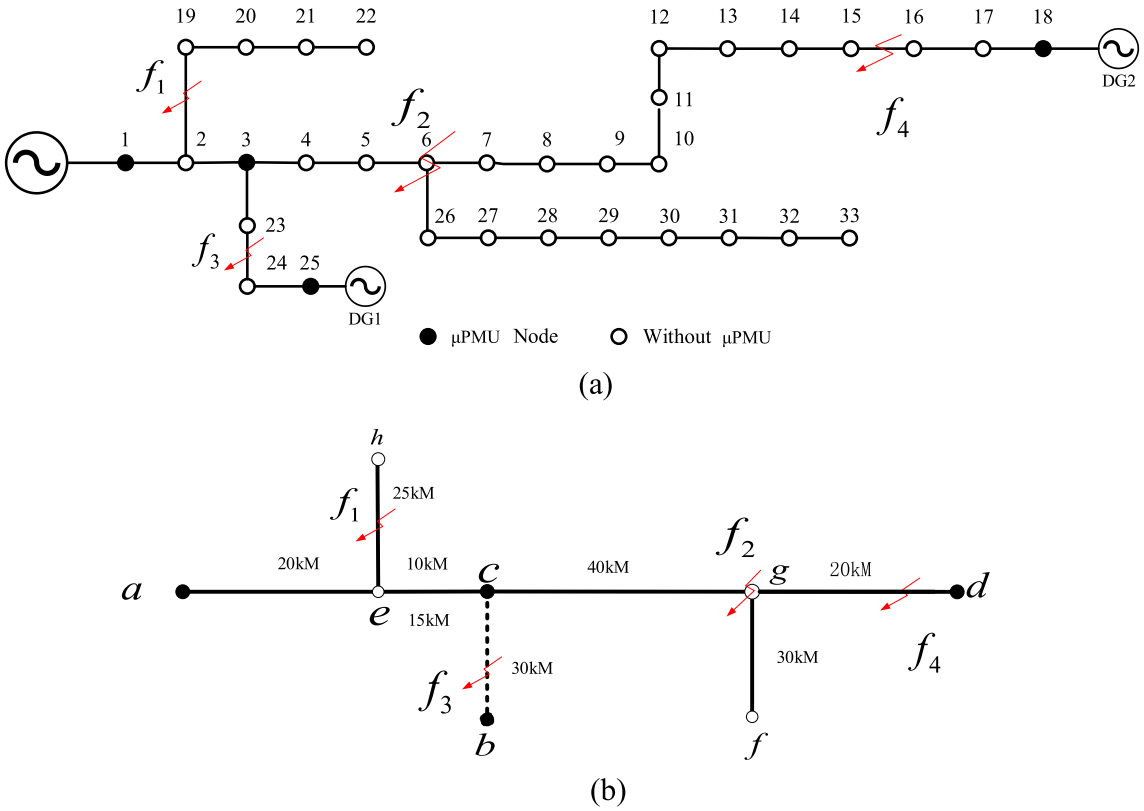

Fig. 6 The 10 kV overhead line-cable hybrid structure of distribution network topology: **a** standard IEEE 33 node 10 kV distribution network; **b** simplified diagram of simulation model

Table 1 Section lengths

Section	*ae*	*eh*	*ec*	*bc*	*cg*	*gf*	*gd*
Length/km	20	40	10	30	40	30	20

Table 2 Section lengths

Fault type	f_1	f_2	f_3	f_4
Fault distance/km	15	20	25	15
Reference node	*e*	*d*	*c*	*d*

data in Table 1. Then, the inherent time matrix (T_d) is calculated between valid nodes by v_1.

$$D = \begin{array}{c} \\ a \\ b \\ c \\ d \\ e \\ f \\ g \\ h \end{array} \begin{array}{c} \begin{array}{cccccccc} a & b & c & d & e & f & g & h \end{array} \\ \begin{bmatrix} 0 & 60 & 30 & 80 & 20 & 100 & 70 & 60 \\ 60 & 0 & 30 & 80 & 40 & 100 & 70 & 60 \\ 30 & 30 & 0 & 50 & 10 & 70 & 40 & 50 \\ 80 & 80 & 50 & 0 & 60 & 40 & 10 & 100 \\ 20 & 40 & 10 & 60 & 0 & 80 & 50 & 40 \\ 100 & 100 & 70 & 40 & 80 & 0 & 30 & 120 \\ 70 & 70 & 40 & 10 & 50 & 30 & 0 & 90 \\ 60 & 60 & 50 & 100 & 40 & 120 & 90 & 0 \end{bmatrix} \end{array} \tag{19}$$

$$T_d = \frac{D}{v_1} = \begin{array}{c} \\ a \\ b \\ c \\ d \end{array} \begin{array}{c} \begin{array}{cccc} a & b & c & d \end{array} \\ \begin{bmatrix} 0 & 2.004 & 1.002 & 3.006 \\ 2.004 & 0 & 1.002 & 3.006 \\ 1.002 & 1.002 & 0 & 2.004 \\ 3.006 & 3.006 & 2.004 & 0 \end{bmatrix} \end{array} \times 10^{-4} \tag{20}$$

4.1 Fault simulation

Different types of fault simulations are carried out to verify the effectiveness and reliability of the proposed method. Faults f_1 to f_4 are set in the distribution network to represent the faults in the invalid branch, the valid section, the proportion with inverter-based distributed generation (IBDG) and the one with a doubly fed induction generator (DFIG), respectively. The initializing fault distances are set as shown in Table 2. The fault occurs at 0.035 s, the simulation time is 0.1 s, and the sampling frequency is set as 1 MHz. The simulation results are as follows.

Case 1: Faults on invalid branches between valid nodes A fault f_1 occurs on the branch *eh*. First, the simulation data are imported from PSCAD into MATLAB, and the B spline wavelet is used to obtain the modulus maximum of the wavelet transform at the 6th scale. The simulation results are shown in Fig. 7, where the red dots are used to calibrate the arrival time of the traveling wave heads.

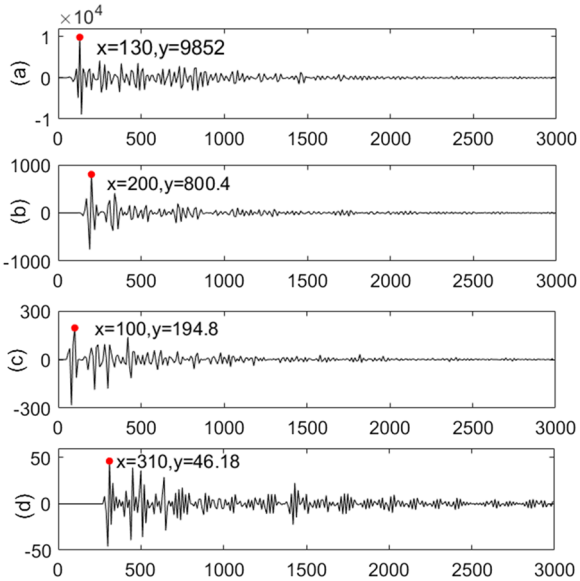

Fig. 7 The simulation results of traveling wave heads arriving at valid nodes

Establish T_f according to the arriving time when the fault traveling waves reach to each detection devices, as:

$$T_f = \begin{array}{c} \\ a \\ b \\ c \\ d \end{array} \begin{array}{c} \begin{array}{cccc} a & b & c & d \end{array} \\ \begin{bmatrix} 0 & 3.007 & 2.005 & 4.009 \\ 3.007 & 0 & 2.673 & 4.677 \\ 2.005 & 2.673 & 0 & 5.011 \\ 4.009 & 4.677 & 5.011 & 0 \end{bmatrix} \end{array} \times 10^{-4} \tag{21}$$

Then, based on T_d and T_f, the time determination matrix ΔT_1 of the fault section is calculated according to:

$$\Delta T_1 = T_f - T_d$$

$$\Delta T_1 = \begin{array}{c} \\ a \\ b \\ c \\ d \end{array} \begin{array}{c} \begin{array}{cccc} a & b & c & d \end{array} \\ \begin{bmatrix} 0 & 1.003 & 1.003 & 1.003 \\ 1.003 & 0 & 1.670 & 1.670 \\ 1.003 & 1.670 & 0 & 3.006 \\ 1.003 & 1.670 & 3.006 & 0 \end{bmatrix} \end{array} \times 10^{-4} \tag{22}$$

As shown in ΔT_1 in Eq. (22), all elements are greater than 0 except the diagonal ones. Thus, the fault occurs on an invalid branch in the valid section. The smallest and equal values of elements in ΔT_1 are referred to section *ac*. Therefore, the fault f_1 occurs on the branch *eh* of section *ac*. Finally, the accurate fault position is calculated via Eq. (23), and the error rate e_f of fault location is calculated by Eq. (24).

$$\begin{aligned} d_f &= \frac{1}{2} * \Delta T_{\min} * v_1 = 0.5 \times 0.1003 \times 2.9939 \times 10^2 \\ &= 15.0144\,(\text{km}) \end{aligned} \tag{23}$$

$$e_f = \frac{d_f}{d} = \frac{|15 - 15.0144|}{15} \times 100\% = 0.096\% \tag{24}$$

Case 2: Faults at valid sections A fault f_2 occurs on node g at valid section cd. Based on the simulation data, the wave head arrival times are obtained while $T_f^{'}$ and ΔT_2 are calculated by:

$$T_f^{'} = \begin{array}{c} \\ a \\ b \\ c \\ d \end{array} \begin{array}{c} \begin{array}{cccc} a & b & c & d \end{array} \\ \begin{bmatrix} 0 & 4.676 & 3.674 & 3.006 \\ 4.676 & 0 & 3.674 & 3.006 \\ 3.674 & 3.674 & 0 & 2.004 \\ 3.006 & 3.006 & 2.004 & 0 \end{bmatrix} \end{array} \times 10^{-4} \tag{25}$$

$$\Delta T_2 = T_f^{'} - T_d$$

$$\Delta T_2 = \begin{array}{c} \\ a \\ b \\ c \\ d \end{array} \begin{array}{c} \begin{array}{cccc} a & b & c & d \end{array} \\ \begin{bmatrix} 0 & 2.672 & 2.672 & 0 \\ 2.672 & 0 & 2.672 & 0 \\ 2.672 & 2.672 & 0 & 0 \\ 0 & 0 & 0 & 0 \end{bmatrix} \end{array} \times 10^{-4} \tag{26}$$

Equation (26) shows that values of elements in ΔT_2 referring to section cd are 0, and the remaining ones are greater than 0. Therefore, it detects that the fault occurs within section cd because of the non-zero value of t_{f_c} and t_{f_d}. From the times t_{f_c}, t_{f_d} and t_{f_b}, the accurate fault location is calculated by Eq. (27), while d is the reference node.

$$\begin{cases} d_1 = \frac{t_{f_d}}{t_{f_d} + t_{f_c}} * d_{cd} \\ d_2 = \frac{t_{f_d}}{t_{f_d} + t_{f_b}} * d_{bd} \\ d^* = \frac{d_1 + d_2}{2} \end{cases} \tag{27}$$

According to the calculation results, it detects that the fault occurs at section cd, which is located 20.0285 km from the reference node d. Compared with preset conditions, the fault section identification is accurate, and the error of fault distance is 0.0285 km and error rate is 0.1425%. This satisfies the calculation accuracy requirements.

Case 3: Faults at DG sections A 3 MW IBDG and a 3 MW DIFG are set on node b and d, respectively. Assuming the faults f_3 and f_4 occur in section bc and gd, respectively, the specific simulation results based on the proposed method are shown in Table 3. Table 3 shows that the fault section identification results are accurate with different types of DGs. The errors of fault distances are 0.0716 km with IBDG and 0.0240 km with DIFG, respectively, i.e., with respective error rates of 0.286% and 0.160%. The results show that the proposed method can be adapted to different types of DG.

Table 3 Simulation results of fault location with DG

Fault type	DG type	Fault section	Results/km	Error/km	Error rate/%
f_3	IBDG	*bc*	25.0716	0.0716	0.286
f_4	DIFG	*gd*	14.9760	0.0240	0.160

4.2 Analysis of simulation results

Further studies have been carried out to verify the effectiveness of the proposed method under different conditions.

(a) *Different transition resistance* The simulation results of fault location with different transition resistances, shown in Table 4, indicate that when the transition resistance increases from 10 to 500, their influence on the accuracy of fault location increases linearly. For sections *cd* and *eh*, their fault location errors increase 0.834% and 1.424%, respectively. Similarly, for sections *bc* and *gd* with different types of DG, their fault location errors increase 0.969% and 1.078%, respectively. Considering that the short circuit fault in the actual power system is mainly the transient grounding fault with low transition resistance, the proposed method still has good engineering application value.

(b) *Comparisons with other two methods* To show the high efficiency and practicality of the proposed method, we carry out comparisons between the proposed method and two other traveling wave-based methods in [27] and [30]. The single-phase-to-earth faults f_3 and f_4 with 10 Ω fault impedance and 15° fault inception angle are simulated based on the IEEE 33-node system. An IBDG and a DIFG is set at nodes *b* and *d*, while the detection devices are set at nodes a, b, c and d. Table 5 shows that all three methods have good location accuracy. The method in [27] has good accuracy of fault location, but it cannot deal with the fault f_1 without a detection device on the invalid branch *eh*. The method in [30] can effectively locate faults in the optimal configuration of detection devices, although it cannot adapt to the proportion of DGs, and the location error rates of faults f_3 and f_4 are higher than 2%. The results show that compared with the other two methods, the proposed method can locate the faults accurately under different conditions. When the proposed method considers the different types of DG and the optimal configuration of detection devices, the location error rates are all lower than 0.5%.

Table 4 Simulation results of fault location with different transition resistances

DG type	Transition resistance/Ω	Fault section	Results/km	Error/km	Error rate increased/%
–	10	*cd*	20.0285	0.0285	0.834
	50	*cd*	20.0399	0.0399	
	100	*cd*	20.1025	0.1025	
	500	*cd*	20.1952	0.1952	
–	10	*eh*	15.0144	0.0144	1.424
	50	*eh*	15.1221	0.1221	
	100	*eh*	14.8954	0.1046	
	500	*eh*	15.2280	0.2280	
IBDG	10	*bc*	25.0716	0.0716	0.969
	50	*bc*	25.0827	0.0827	
	100	*bc*	25.1102	0.0902	
	500	*bc*	25.3139	0.3139	
DIFG	10	*gd*	14.9760	0.0240	1.078
	50	*gd*	15.0219	0.0219	
	100	*gd*	15.0941	0.1102	
	500	*gd*	15.1838	0.1838	

Table 5 Comparison results of fault location

Methods	Fault type	Error rate/%			
		f_1	f_2	f_3	f_4
[27]	Ag	–	0.159	0.227	0.303
[30]	Ag	0.115	0.172	2.390	2.272
Proposed method	Ag	0.096	0.143	0.286	0.160

Table 6 Simulation results with time error

Fault type	Time error (μs)	Results/km	Error/km	Error rate increased (%)
f_1	0	20.0285	0.0285	0.057
	0.2	20.0399	0.0399	
f_2	0	15.0144	0.0144	0.432
	0.2	15.0799	0.0792	
f_3	0	25.0716	0.0716	0.106
	0.2	25.0981	0.0981	
f_4	0	14.9760	0.0240	0.087
	0.2	14.9627	0.0373	

(c) *Time detection error* There are various disturbances in practice, such as time sampling error, which may lead to a certain deviation of the time of collection. To improve the simulation accuracy, 0.2 μs time error is added to the data collected, and the simulation results with different fault types with time errors are shown in Table 6.

As seen, the proposed method can achieve fast and effective fault location for the faults occurring on valid and invalid branches. In the optimal configuration of detection devices of traveling waves with the time error of 0.2 μs, the fault location error rates only increase 0.057% and 0.380% for faults f_1 and f_2, respectively. The error rates increase 0.106% and 0.087% for fault types f_3 and f_4 under the proportion of DGs, respectively, which still satisfies engineering requirements. Therefore, the proposed method is robust to a certain amount of time errors and can effectively improve engineering practicability.

5 Conclusion

To achieve accurate location of faults in distribution networks at low cost, this paper proposes a novel method based on the time matrix of traveling waves in an optimal device configuration. It is effective for both ideal and optimal configuration conditions. The initial wave head data of traveling waves are extracted to establish the time determination matrix, and this realizes fault section identification and fault distance calculation. The good robustness of the proposed method to DGs, transition resistance and time detection error are also verified. Simulation results demonstrate that the proposed method is effective with high accuracy for fault location under different fault conditions. To meet the needs of new power grids, fault location of distribution networks with a high proportion of DGs will be the subject of future work.

Abbreviations
DG: Distributed Generators; IDM: Inherent Distance Matrix; ITM: Inherent Time Matrix; TDM: Time Determination Matrix; IBDG: Inverter Based Distributed Generation; DFIG: Doubly Fed Induction Generator.

Acknowledgements
This research was partially funded by grants from the National Natural Science Foundation of China (61703345), the Chunhui Project Foundation of the Education Department of China (Z201980), the Open Research Subject of Key Laboratory of Fluid and Power Machinery (Xihua University), Ministry of Education (szjj2019-27).

Author contributions
Formal analysis: LC; Investigation: LC; Supervision: TW; Writing—original draft: LC; Writing—review and editing: TW; Data curation: WY. All authors have read and approved the final manuscript.

Funding
There is no external funding.

Availability of data and materials
Data and materials are obtained simulation program. This simulation program is PSCAD/MATLAB.

Declarations

Competing interests
The authors declare that they have no known competing financial interests or personal relationships that could have appeared to influence the work reported in this paper.

Author details
[1]School of Electrical Engineering and Electronic Information, Xihua University, Chengdu 610039, China. [2]Key Laboratory of Fluid and Power Machinery, Ministry of Education, Xihua University, Chengdu 610039, China.

Received: 19 April 2022 Accepted: 24 October 2022
Published online: 17 November 2022

References

1. Wang, T., Liu, W., Luis, V. C., et al. (2022). A novel fault diagnosis method of smart grids based on memory spiking neural P systems considering measurement tampering attacks. *Information Sciences, 596*, 520–536.
2. Li, Z. X., Wan, J. L., Wang, P. F., et al. (2021). A novel fault section locating method based on distance matching degree in distribution network. *Protection and Control of Modern Power Systems, 6*(2), 253–263.
3. Pignati, M., Zanni, L., Romano, P., et al. (2017). Fault detection and faulted line identification in active distribution 18 networks using synchro-phasors-based real-time state estimation. *IEEE Transactions on Power Delivery, 26*(2), 381–392.
4. Li, C. C., Xi, Y. N., Lu, Y. F., et al. (2022). Resilient outage recovery of a distribution system: Co-optimizing mobile power sources with network structure. *Protection and Control of Modern Power Systems, 7*(3), 459–471.
5. Chen, K., Huang, C., & He, J. (2016). Fault detection, classification and location for transmission lines and distribution systems: A review on the methods. *High Voltage, 1*(1), 25–33.
6. Jamali, S., Bahmanyar, A., & Ranjbar, S. (2020). Hybrid classifier for fault location in active distribution networks. *Protection and Control of Modern Power Systems, 5*(1), 17.
7. Dashti, R., Daisy, M., Shaker, H. R., et al. (2018). Impedance-based fault location method for four-wire power distribution networks. *IEEE Access, 6*, 1342–1349.
8. Teng, J. H., Huang, W. H., & Luan, S. W. (2014). Automatic and fast faulted line-section location method for distribution systems based on fault indicators. *IEEE Transactions on Power Systems, 29*(4), 1653–1662.
9. Pasdar, M., Sozer, Y., & Husain, I. (2013). Detecting and locating faulty nodes in smart grids based on high frequency signal injection. *IEEE Transactions on Smart Grid, 4*(2), 1067–1075.
10. Niu, L., Wu, G., & Xu, Z. (2021). Single-phase fault line selection in distribution network based on signal injection method. *IEEE Access, 9*, 21567–21578.
11. Xie, L., Luo, L., Li, Y., et al. (2020). A traveling wave-based fault location method employing VMD-TEO for distribution network. *IEEE Transactions on Power Delivery, 35*(4), 1987–1998.
12. Shi, S., Lei, A., He, X., et al. (2018). Travelling waves-based fault location scheme for feeders in power distribution network. *The Journal of Engineering, 2018*(15), 1326–1329.
13. Xi, Y., Li, Z., Zeng, X., et al. (2018). Fault location based on travelling wave identification using an adaptive extended Kalman filter. *IET Generation Transmission & Distribution, 12*(6), 1314–1322.
14. Chen, W. H. (2011). Fault section estimation using fuzzy matrix-based reasoning methods. *IEEE Transactions on Power Delivery, 26*(1), 205–213.
15. Chen, K. J., Hu, J., Zhang, Y., et al. (2019). Fault location in power distribution systems via deep graph convolutional networks. *IEEE Journal on Selected Areas in Communications, 38*(1), 119–131.
16. Zhang, T., Sun, L. X., Liu, J. C., et al. (2018). Fault diagnosis and location method for active distribution network based on artificial neural network. *Electric Power Components and Systems, 46*(9), 987–998.
17. Lin, S., He, Z. Y., Li, X. P., et al. (2012). Travelling wave time frequency characteristic-based fault location method for transmission lines. *IET Generation, Transmission & Distribution, 6*(8), 764–772.
18. Xi, Y., Zhang, X., Li, Z., et al. (2018). Double-ended travelling-wave fault location based on residual analysis using an adaptive EKF. *IET Signal Processing, 12*(8), 1000–1008.
19. Goudarzi, M., Vahidi, B., Naghizadeh, R. A., et al. (2015). Improved fault location algorithm for radial distribution systems with discrete and continuous wavelet analysis. *International Journal of Electrical Power & Energy Systems, 67*, 423–430.
20. Lopes, F. V., Fernandes, D., & Neves, W. L. A. (2013). A traveling-wave detection method based on Park's transformation for fault locators. *IEEE Transactions on Power Delivery, 28*(3), 1626–1634.
21. Bernadic, A., & Leonowicz, Z. (2012). Fault location in power networks with mixed feeders using the complex spacephasor and Hilbert-Huang transform. *International Journal of Electrical Power & Energy Systems, 42*(1), 208–219.
22. Lee, Y. J., Chao, C. H., Lin, T. C., et al. (2018). A synchrophasor-based fault location method for three-terminal hybrid transmission lines with one off-service line branch. *IEEE Transactions on Power Delivery, 33*(6), 3249–3251.
23. Lopes, F. V., Dantas, K. M., Silva, K. M., et al. (2018). Accurate two-terminal transmission line fault location using traveling waves. *IEEE Transactions on Power Delivery, 33*(2), 873–880.
24. Hu, M. F., Liu, Y., & Hua, B. (2021). Distributed fault location for distribution networks under optimal configuration of measuring devices. *Power System Technology, 45*(07), 2616–2622.
25. Liwei, X., Yong, L., Longfu, L., Chun, C., & Yijia, C. (2020). Fault location method for distribution networks based on distance matrix and branch coefficient. *Proceedings of the CSEE, 40*(07), 2180–2191.
26. Kumar, R., & Saxena, D. (2019). Fault location in distribution network using travelling waves. *International Journal of Energy Sector Management, 13*(3), 651–669.
27. Deng, F., Li, X. R., Zeng, X. J., et al. (2018). A novel multi-terminal fault location method based on traveling wave time difference for radial distribution systems with distributed generators. *Proceedings of the CSEE, 38*(15), 4399–4409.
28. Li, Z. W., Yi, Z. P., Yang, Y., et al. (2015). Optimal placement of traveling wave fault location equipment for power grid based on genetic algorithm. *Power System Protection and Control, 43*(3), 77–83.
29. Tashakkori, A., Wolfs, P. J., Islam, S., et al. (2020). Fault location on radial distribution networks via distributed synchronized traveling wave detectors. *IEEE Transactions on Power Delivery, 35*(3), 1553–1562.
30. Chen, R., Yin, X., Yin, X. G., et al. (2019). Computational fault time difference-based fault location method for branched power distribution networks. *IEEE Access, 7*, 181972–181982.